PAPER • **OPEN ACCESS**

Design Loads in Small Wind Turbines: a Detailed Comparison Between Pitch and Stall Regulation

To cite this article: F Papi *et al* 2022 *J. Phys.: Conf. Ser.* **2385** 012120

Design Loads in Small Wind Turbines: a Detailed Comparison Between Pitch and Stall Regulation

F Papi*, L Pagamonci, A Bianchini

Department of Industrial Engineering, Università degli Studi di Firenze. Via di Santa Marta 3, 50139, Firenze, Italy

*fr.papi@unifi.it

Abstract Small wind turbines (SWTs) have known alternate fortune but can now play a key role in distributed production to foster energy transition. Among the typical features of small machines, the use of stall regulation is a distinctive one, since the ubiquitous variable speed pitch regulation used in utility-scale rotors is hampered by space constraints in small nacelles. This reduced the cost and boosts overall reliability; on the other hand, compromises in the aerodynamic design of the blades must be adopted to ensure smooth power regulation above rated windspeed. This has implications not only on the final Annual Energy Production (AEP) of the rotors, but also on loads. The current study aims at investigating the differences in peak loads between a stall and a pitch regulated SWT. The UNIFI 50kW SRWT, a reference turbine designed by Università degli Studi di Firenze, is used as a case study thanks to the fact that is available both with stall and pitch control options. Differently from most of the studies to date, simulations are carried out for a variety of power production and parked load cases, significant for extreme loading of the rotor and tower of the wind turbine, thus strongly impacting on the design. Results demonstrate how a pitch-regulated machine can ensure a significant reduction of the main maximum loads, thus paving the way for more optimized and cost-effective designs of future SWTs.

1. Introduction

Interest is nowadays building up once again around small wind turbines (SWTs) [1]. These machines, most of which generally have a power output lower than 50-60 kW, have known alternate fortune over the years, also due to the intermittent incentives offered for their deployment by governments all over the world. Today, however, there is at least ~1.8 GW of installed small wind capacity globally from over 1 million turbines [2], which play a key role in providing sustainable energy to many off-grid and rural systems [3]. Looking to near future, SWTs are considered as an important element of the future distributed energy networks, especially if a more effective combination with storage systems will be ensured [4]; challenges still need to be addressed, however, to reduce their Levelized Cost of Energy and therefore improve competitiveness with respect to other renewables [1]. Focusing on design, horizontal-axis SWTs have not converged to a consolidated archetype (this indeed representing one of the main factors hampering a faster industrial development); on the other hand, they have some distinctive features that make the unique in comparison to utility-scale machines. For example, for small rated-power values (10 kW or less), some form of free or passive yaw is typically used. The most popular options are then a tail fin or the use of a downwind rotor. For higher power rates, the use of yaw-drive mechanisms to align the rotor to the mean wind direction like those of utility-scale turbine are used. For these applications, however, differences are still present both in blade aeroelastic design and in control. In particular, while variable speed pitch regulation has emerged as the only method of power regulation in utility-scale turbines, this regulation method is hampered in SWTs by cost, mostly, by space constraints in the small nacelles. Therefore, stall regulation is often preferred [5], as manufacturers can

make it without a blade pitch system, greatly reducing installation cost and boosting overall reliability. However, some compromises in the aerodynamic design of the blades must be adopted when designing a stall regulated wind turbine. In fact, designers are often forced to compromise on peak performance, to ensure smooth power regulation above rated windspeed. Therefore, from an energy capture standpoint, stall regulation often causes lower Annual Energy Production (AEP), as investigated in [6]. The lack of a blade pitching system has implications in the turbine loading too. For instance, in very high wind speeds, where the wind turbine is parked for safety causes, blades are typically pitched to 90° in a pitch-regulated wind turbine, greatly reducing the angle of attack and resulting loads [7]. In stall regulated wind turbines, the blade pitch angle is fixed, leading to very high blade loads in parked conditions. On the other hand, small wind turbines have very low inertia, and they pick up or shed rotational speed very quickly in the highly turbulent environments they operate in. Consequently, the blade pitch controller may not be able to keep up, leading to less tightly controlled rotor speed above rated wind speed.
The present study aims at investigating the differences in peak loads between stall- and pitch-regulated SWTs. The UNIFI 50kW SRWT, a reference turbine designed by the Università degli Studi di Firenze (Section 2), is used as a case study thanks to the fact that is available both with stall and pitch control options. Simulations according to international design standard specification [8] are carried out for a variety of power production and parked load cases, significant for extreme loading of the rotor and tower of the wind turbine (Section 3). Most studies to date in fact concentrate on load comparison in power-production conditions. Such a comparison however is non-exhaustive, as extreme, design-driving, loads depend on other design situations, which may vary based on the regulation strategy (pitch or stall). To the best of the authors' knowledge, such a quantitative and qualitative comparison has not been performed to date. Peak loads for the pitch- and stall-regulated machines are compared and discussed (Section 4) to highlight the differences in estimated loads. Some final conclusions on the prospects for the introduction of pitch regulation in SWTs are finally drawn in Section 5.

2. Case study

The UNIFI 50kW RWT has been selected as the case study for this work. It is a 50kW reference turbine (Figure 1) recently developed by Università degli Studi di Firenze. The turbine has a 200 m^2 swept rotor area. Its main design and performance parameters are resumed in Table 1. Differently from other similar models in the literature, this turbine is available in two versions, i.e. both the pitch-controlled, and the stall-controlled one, each of which having its corresponding control and tower configurations. Open-source access to geometry files, turbine properties' data, OpenFAST [9] models and control algorithms is provided at the following GitHub space https://github.com/UNIFI 50kW RWT. For the purposes of the present study, it is worth noting that the turbine has been originally designed using airfoil polars extrapolated with the Montgomerie method [10] and corrected for rotational-augmentation with the Bak's method [11]. The reader is referred to the GitHub repository for any additional detail about the turbine; a detailed explanation of the variable speed, stall-control strategy can be also found in [12].

Table 1. UNIFI 50kW RWT specifications.

Parameter	Value
IEC wind class	II A
Rotation axis	Horizontal
Number of blades	3
Rotor diameter	16 m
Hub radius	0.5 m
Rated Power	50 kW
Control	Pitch and/or stall
Cut-in/Cut-out wind speed	3.2 - 20 m/s
Rated wind speed	12 m/s
Hub height	25 m
Airfoil family	NREL S821-19-20

Figure 1. UNIFI 50kW RWT.

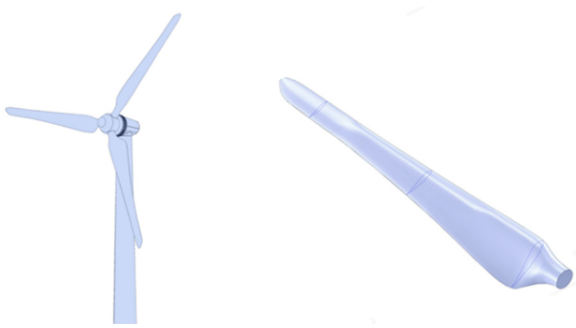

3. Methods

Turbine performance and loads have been calculated using OpenFAST [4], an open-source modular tool developed by the National Renewable Energy Laboratory (NREL) for the modelling of the aero-servo-elastic response of wind turbines. The code has been widely adopted, validated, and used in the design of multiple, industry-standard, reference wind turbines (e.g., [13][14]). In the present study, aerodynamics are modelled using the Blade Element Momentum (BEM) theory with corrections for wind shear, yaw misalignment, tip and hub losses, and tower-shadow effects, as implemented in AeroDyn. Dynamic stall is treated with the Beddoes–Leishman dynamic stall model, also included in the AeroDyn module. This correction is especially relevant for a stall-regulated turbine operating in turbulent conditions. The structural behavior is modelled with the ElastoDyn module, while the turbine controller was integrated through the ServoDyn module. For the pitch-controlled turbine, an external routine was used, as detailed in the following.

For the calculation of peak loads, significant Design Load Cases (DLCs) from the ones prescribed by the International Electrotechnical Commission (IEC) 61400-2 [3] have been chosen, in the attempt to investigate the most frequent operational points or the most extreme events. The selected DLCs include power production conditions and parked conditions with and without the occurrence of faults. Faults occurring during power production are disregarded. Table 1 and Table 2 describe the selected load cases for the stall-regulated and the pitch-regulated machines, respectively. For turbulent simulations, multiple seeds of wind fields have been generated in order to account for the stochastic effect of turbulence on the instantaneous wind speed, including Normal Turbulence Model (NTM), Extreme Coherent Gust with Direction Change (ECD), or Extreme Wind Models (EWM) in 1 or 50 years. More specifically, DLC 1.1 corresponds to normal operating conditions in terms of wind speed and turbulence, with wind speeds between cut-in (3 m/s) and cut-off (20 m/s) conditions of the selected turbine. Considering the 2 m/s binning, the number of seeds for each bin, the 3 wind directions analyzed to account for yaw misalignment, and a simulation time of 10 minutes for each simulation, a total real time of 27 hours is simulated. DLC 1.2 instead analyzes the behavior of the turbine under an extreme gust with a simultaneous direction change: in this case, no seeds are required, but two different simulations are performed, according to the two possible direction changes. DLC 5.1 and DLC 5.2 consider a situation of parked rotor during a condition of extreme wind loading, under a maximum wind speed with a 50-year recurrence period and with a 1-year recurrence period (wind speed equal to 70% of the previous value). Finally, DLC 6.1 simulates a parked and fault conditions under a wind speed with a 1-year recurrence period. A partial safety factor of 1.35 is applied to all the output loads. It is worth noting that, according to the selected control strategy, some differences on the setup of the simulations are apparent. For DLC 5.1, a pitch angle of 90° has been set for the pitch regulated machine, consistently with the "parked" configuration of these rotors, upon which a yaw misalignment of +/- 15° is added.

Table 2. Summary of IEC DLC Settings for the stall-regulated machine.

DLC	Wind condition	Wind speeds	Yaw angles	Vertical inflow angle	# of seeds	# of simulations	Total simulated time
1.1	NTM	3:2:19 m/s	0/+8/-8 deg	-8 deg	6	162	27 h
1.2	ECD	12 m/s	0 deg	-8 deg	-	2	400 s
5.1	EWM50	43 m/s	-105/-75 deg	-8 deg	6	6	1 h
5.2	NTM	30 m/s	-82 deg	-8 deg	6	6	1 h
6.1	EWM1	30 m/s	0 deg	-8 deg	6	24	8 h

Table 3. Summary of IEC DLC Settings for the pitch-regulated machine.

DLC	Wind condition	Wind speeds	Yaw angles	Vertical inflow angle	# of seeds	# of simulations	Total simulated time
1.1	NTM	3:2:19 m/s	0/+8/-8 deg	-8 deg	6	108	18 h
1.2	ECD	12 m/s	0 deg	-8 deg	-	2	400 s
5.1	EWM50	43 m/s	+15/-15 deg	-8 deg	6	6	1 h
5.2	NTM	30 m/s	+8 deg	-8 deg	6	6	1 h
6.1	EWM1	30 m/s	0 deg	-8 deg	6	6	8 h

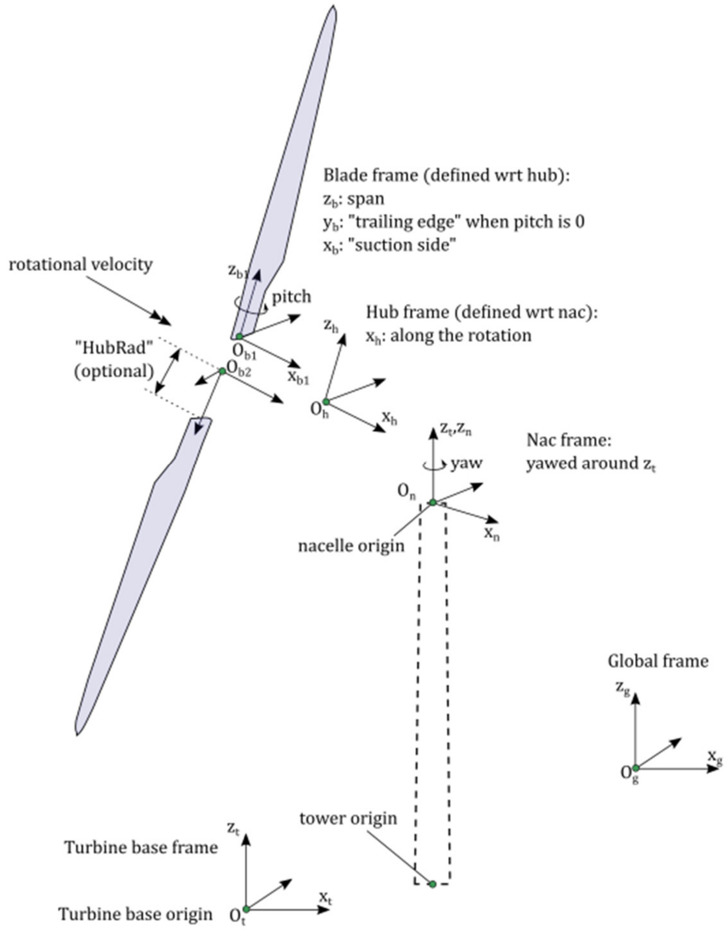

Figure 2. Turbine reference frame adopted in OpenFAST [9]

These values turn into yaw misalignments of -105° and -75°, respectively, for the stall-regulated turbine, which is not able to feather the blades, and is therefore yawed out of the wind when parked. The same applies for DLC 5.2, where the stall regulated machine has a -82° yaw misalignment, which becomes equal to +8° for the pitch-regulated machine. For DLC 6.1 instead two different approaches have been adopted for the stall- and the pitch-regulated turbines. For the first one, which is parked with the mechanical brake inserted, four different azimuthal positions have been set (0°/30°/60°/90°); considering that a three-bladed turbine is being analyzed, this allows to simulate the machine in every azimuthal position with a 30° spacing. On the other hand, the pitch-controlled turbine, which is parked in idling with the blades pitched to feather, was accordingly let free to rotate. Finally, for both turbines a slowly changing wind direction around the rotor has been imposed, in order to fully investigate the rotor structural behavior for the full range of yaw misalignment during fault conditions. MExtremes [15], a set of MATLAB® scripts developed by NREL, has been chosen for the post-processing of the results. This software indeed allows to generate extreme-event tables for one or more time series. In particular, attention has been given to the extrapolation of forces and moments acting on the root of the blades, on the top/base of the tower, and on the drivetrain. The methodology followed by MExtremes to calculate extreme loads is the one prescribed by the IEC 61400-2 standards [8], corresponding to the so-called "averaging approach". The characteristic maximum and minimum loads are calculated as the mean of the maximum and the minimum of all stochastic realizations (i.e. "seeds"), respectively. An important feature of this program is that not only a qualitative analysis of the peak loads is allowed, but it also gives information on which cases the corresponding loads occur for the two types of machines.

4. Results

To get an insight on the induced differences in loading between the two regulation methods, blade root forces and moments are analyzed first. With reference to Figure 2, which shows the conventions and reference systems, forces in x, y and z in the blade relative frame directions are arranged in order to have the moment caused by edgewise forces about the x_b axis and the moment caused by flapwise forces about the y_b axis. The y_b axis is directed parallel to the blade chord if the twist angle is zero, and the x_b axis is normal to it and directed downwind. This reference system pitches with the blades – an important consideration for the pitch-regulated machine – and is chosen because it gives a good representation of blade design loads. Moreover, in this analysis and in all following ones, the indication of the DLC in which peak loads are registered is displayed, since this will represent a key metrics to compare the two different regulation methods. Moving to results, Figure 3 shows the peak loads at the blade root for both the pitch and the stall regulated turbines. Upon examination of the figure, it is apparent that the loads on the stall machine are generally higher, especially the flapwise moment, which is more than 18% higher with respect to the pitch option. In particular, it is worth analyzing in further detail this latter case for the stall regulated machine. The peak in the flapwise root bending moment is registered in DLC 1.2, which includes a gust and a wind direction change. The combined effect of these two phenomena is apparent in Figure 4 that reports (from the top to the bottom) the moment, generator speed, blade pitch, wind velocity normal and parallel to the rotor plane (if yaw angle was zero) over time in DLC 1.2 for both machines. In particular, one can notice that the stall regulated turbine is not able respond quickly to the shift in wind direction and speed; the angle of attack on the blades is generally increased, leading to strong positive peaks in the moment (i.e., the blade tends to be flexed in the streamwise direction). On the other hand, the pitch regulated turbine responds to the gust by adapting the pitch so to reduce the angle of attack. In this latter case, the simultaneous presence of a yaw angle even leads to negative angles of attack in the outer portions of the blade in some azimuthal positions, which in turn can even generate negative root moments. Moreover, intense peaks are apparent, due again to the high yaw angle the turbine works with and to the interference with the tower.
The only load that is remarkably higher for the pitch regulated machine is the maximum axial force: this result is due to the centrifugal force and its dependency on the quadratic power of the revolution speed, concurrently with a particular condition of revolution speed experienced during normal operating conditions (DLC1.1). As the revolution speed of the pitch-regulated machine is higher, so is the centrifugal force and consequently the axial load.

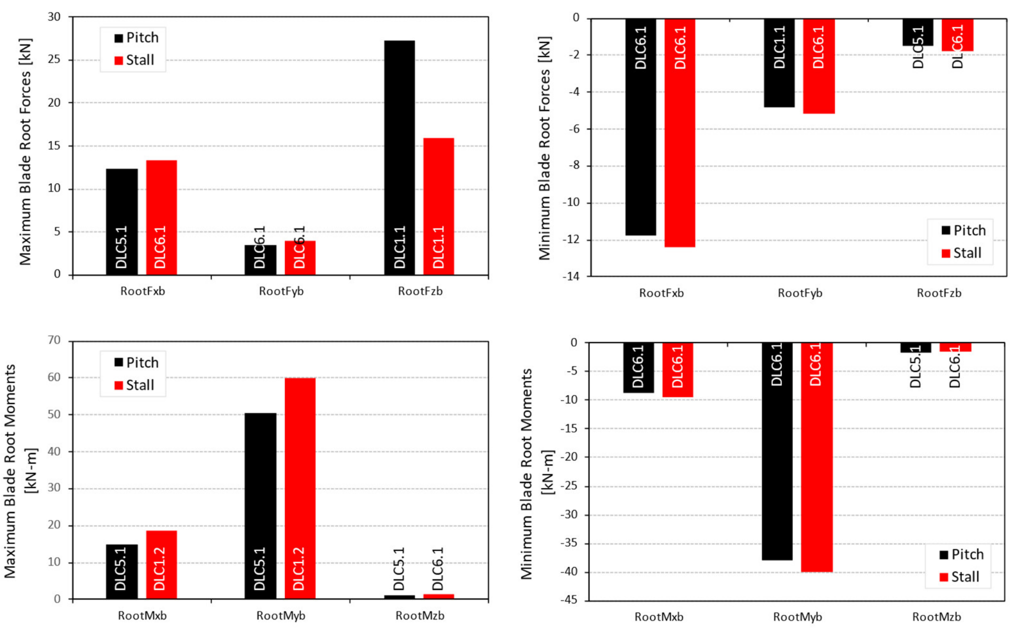

Figure 3. Peak loads at the blade root, comparisons between pitch and stall regulated machines

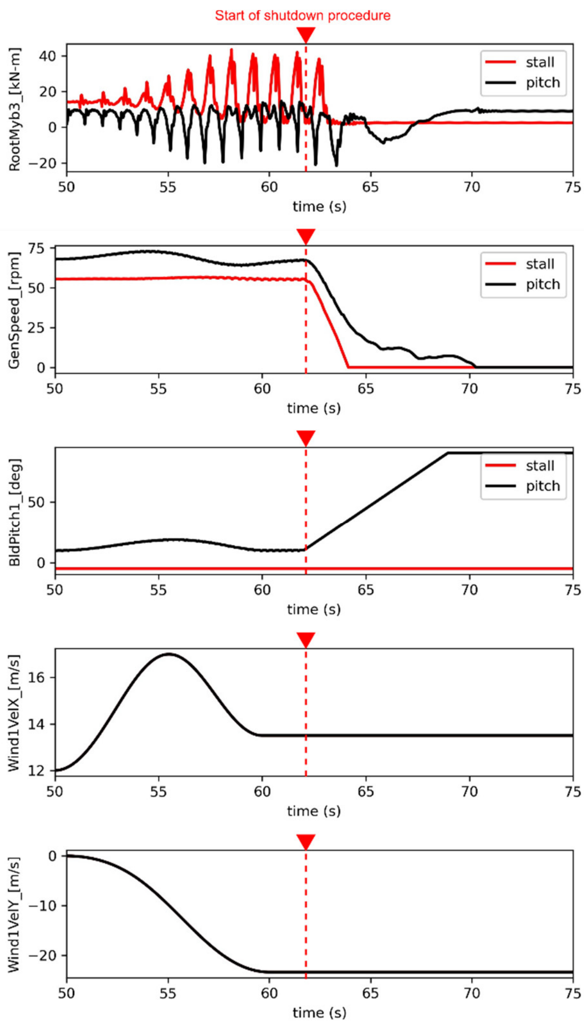

Figure 4. Analysis of the blade root bending moment for the two turbines in DLC 1.2

Looking instead at root forces, peak root flapwise force (RootFxb) is recorded in DLC5.1 for the pitch-regulated machine, while in DLC6.1 for the stall-regulated turbine. In more detail, the mechanism that leads to these extreme values is completely different for the two machines and is worth analyzing in depth, as shown in Figure 5. As discussed, in fact in DLC 5.1 the pitch-regulated rotor is parked facing directly into the wind (with a ±15° yaw error) with feathered blades. The stall machine, on the other hand, is parked with a 90° rotor yaw (again with a ±15° yaw error). Since the blades cannot be feathered in the latter case, they are left in their design setting and the rotor is parked in Y-position (i.e., with one rotor blade pointing vertically downward). For the pitch controlled rotor, the flow impacts the blade with relatively small angles of attack, as shown in Figure 5(sx). Depending on the twist angle of each section and relative yaw error, this leads to high lift forces, especially in root sections that ultimately lead to peaks in RootFxb and in blade root flapwise bending moment (RootMyb). In the stall turbine in Y position, the flow impacts the downward looking blade almost at the trailing edge, leading lo lower lift forces; the upward facing blades are instead subject to very low angles of attack (the blades are facing the wind, which comes almost perpendicular to the revolution axis), again producing a small amount of drag and almost null lift. On the other hand, the stall controlled turbine has the peak in RootFxb in DLC6.1. In this case, due to the loss of grid the flow impacts the blades at a nearly 90° angle, since the rotor directly faces the wind. It is therefore the maximum value of drag force that causes the peak root force in the flapwise direction, as depicted in Figure 5(dx).

Figure 5. Mechanisms leading to peak loads for the pitch- (sx-DLC5.1) and stall-controlled rotor (dx-DLC 6.1)

Overall, we can conclude that the pitch regulation prevents the machine to have dangerous incidence conditions by adapting the blade pitch angle to the new incoming wind direction. Extending these considerations to the whole set of blade loads, one may notice that the pitch regulated machine experiences higher loads during DLC5.1, while DLC6.1 is generally more stressing for the stall one.
Focusing now on the loads at the tower top (Figure 6), more significant differences are noticed between the two turbines, especially for the force on the x direction and for the minimum and maximum values of moments in the x and y direction. For the fore-aft force (YawBrFxp), both peak loads come from DLC6.1, but loads are almost twice as high in the stall machine. Physically speaking, for the stall machine this peak load is generated in the same way as maximum blade-root shear force in the flapwise direction (RootFxb), i.e., 90° flow incidence on the blade in extreme 1-year wind causing high axial loads due to the high drag force. For the pitch machine, on the other hand, maximum loads are recorded when the rotor is at a ± 90° misalignment to the wind. Considering the fact that the blades are feathered in the pitch case, flow incidence is again nearly 90°. The magnitude of the load however is much lower than that in the stall case as only one of the blades is facing the wind at a time. Yaw bearing loads are generally small if compared to tower bottom bending moments, as they are typically caused by aerodynamic imbalances between the blades, which in turn may be caused by a variety of factors, including external ones such as different flow incidence on the three blades (quite common in parked conditions) or wind shear. In more detail, extreme values of the tower-top yaw bearing roll moments (YawBrMxp) and (YawBrMyp) occur for the stall regulated turbine in DLC6.1. For the pitch regulated machine, only the maximum of YawBrMxp takes place during DLC6.1, while the minimum happens during DLC5.1 and the maximum absolute value of YawBrMyp during DLC1.2.
By extending this consideration to a wider point of view, many peak yaw bearing loads come once again from DLC5.1 for the pitch regulated turbine, while DLC6.1 is the most stressing load case for the stall one. At the tower base (Figure 7) the situation is quite different, with similar values of forces in all directions. More importantly, however, the maximum tower base bending moment, which is recorded in the fore-aft direction (TwrBsMyt) is much higher for the stall regulated turbine. This load is often design-driving for the tower itself, therefore a difference such as that observed in Figure 7 is significant. The explanation can be found in what has been noticed at the tower top, as YawBrFxp is converted into a pitch moment at the tower base. Two pieces of evidence support this hypothesis. First, both the yaw bearing fore-aft force and the resulting tower base fore-aft bending moment come from DLC6.1. Secondly, the difference between the pitch moments for the pitch and stall regulated turbines is roughly 400 kN-m, which is coherent with the difference between the two maximum values of YawBrFxp is 20 kN times the flexible tower length is approximately 22 m. In other terms $\Delta_{TwrBsMyt} = \Delta_{YawBrFxp} * H$, with H being the tower height. The most evident difference between the stall and the pitch regulated turbine is apparent in the vertical force TwrBsFzt. This is due to the higher weight of the tower used for this machine with respect to the stall one. As the difference of weight between the two towers is roughly 3400 kg, an additional vertical force of more than 33.2 kN is expected. While not completely general, this result is of interest for a future optimization of SWTs, since the need for a stiffer (and heavier) tower is often needed in the design phase to adapt it to the different resonance frequencies, as discussed in [6].

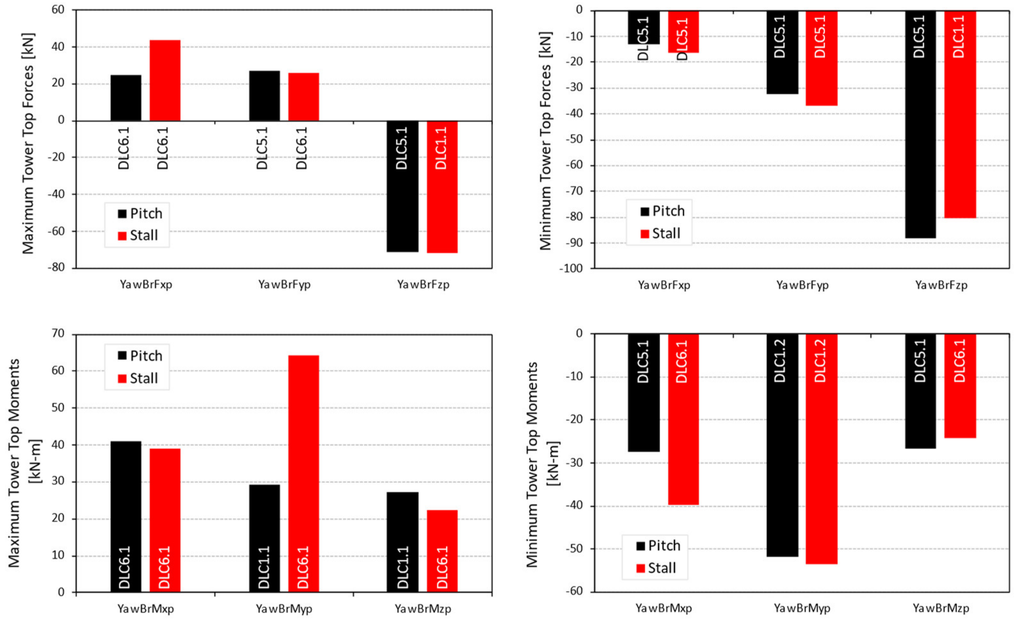

Figure 6. Peak loads at the tower top, comparisons between pitch and stall regulated machines

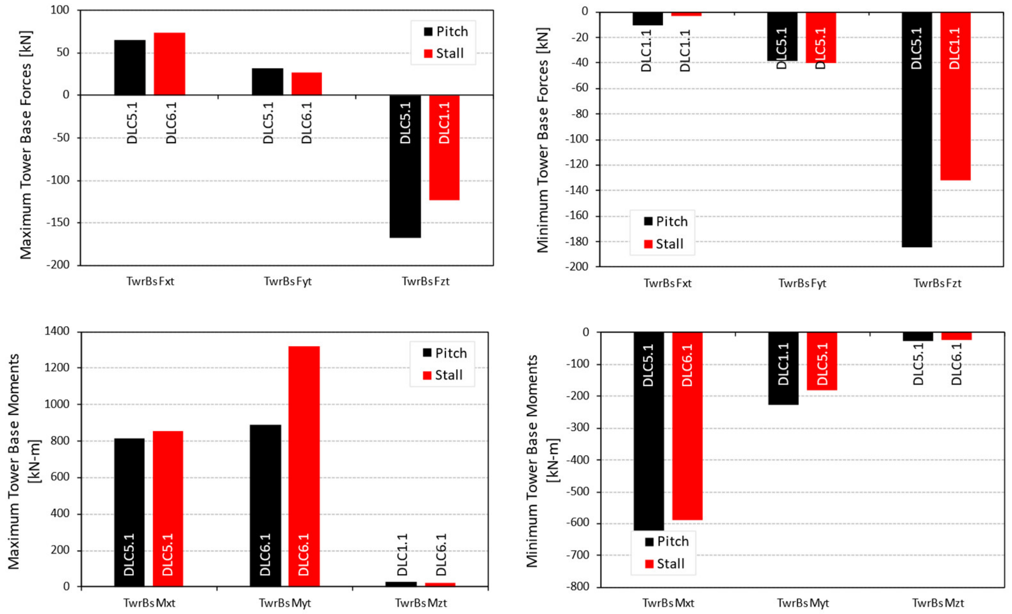

Figure 7. Peak loads at the tower base, comparisons between pitch and stall regulated machines

Together with tower and blades, the drivetrain is an element subject to relevant forces, and so the analysis of the peak loads is worth to be performed, especially for the low-speed shaft directly connected to the rotor (Figure 8). At first glance, loads are notably higher for the stall turbine, particularly in the case of the moment on the x direction, which is more than 250% of the respective value with pitch motion. This is again due to the already discussed mechanism of peak load generation. From a design point of view, this information is anyhow very relevant since can lead to gearbox damage, which accounts for more than 5% of the total turbine cost [1] and represents one of the major sources of downtime periods due to faults [16].

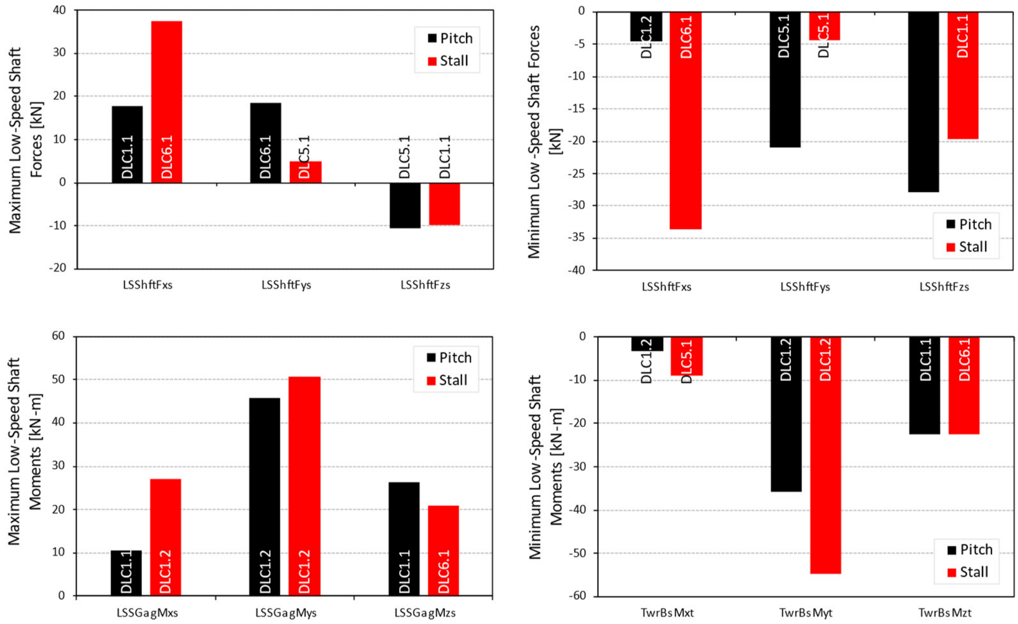

Figure 8. Peak loads at the drivetrain, comparisons between pitch and stall regulated machines

5. Conclusions

In the study, a throughout analysis of the peak loads affecting a small wind turbine is presented, focusing on the differences that may arise in the case it is designed to be either stall- or pitch-regulated. Results showed that there is a significant reduction of the extreme forces and moments acting on blades, tower and drivetrain in case of pitch-regulation, thanks to the fact that the blades can pitched to feather in those DLCs that involve extreme wind conditions and parked rotor, which are often the driving ones in structural design. More specifically, a clear reduction of the flapwise moment is apparent for the blades for the pitch controlled turbine. From a techno-economical perspective, the use of pitch control could potentially allow for the use of less material inside the blade structure, lowering both the cost and the weight. The same can be said for the tower, where a marked decrease in peak fore-aft bending moment is shown. Finally, a notable reduction of the extreme moment acting on the rotor shaft has been observed, with positive potential impacts on the reliability of the gearbox and the whole drivetrain. As a final remark, the present study demonstrates that, beyond the significant increase in the actual energy production discussed recently by some studies, pitch control could lead to significant reduction in peak loads for small wind turbines. Since these are in turn design-driving constraints, the adoption of this control strategy could be payback the additional cost due to the presence of pitch motors, although the lack of space in the nacelle remains an open issue, whose solution is seen as one of the main design advancements needed in the near future.

References

[1] A. Bianchini *et al.*, «Current status and grand challenges for small wind turbine technology», *Wind Energ Sci Discuss*, vol. 2022, pagg. 1–54, giu. 2022, doi: 10.5194/wes-2022-34.
[2] A. C. Orrell, K. Kazimierczuk, and L. Sheridan, «Distributed Wind Market Report: 2021 Edition». 2021. https://www.energy.gov/eere/wind/articles/distributed-wind-market-report-2021-edition-released
[3] C. C. M. Chagas, M. G. Pereira, L. P. Rosa, N. F. da Silva, M. A. V. Freitas, and J. D. Hunt, «From Megawatts to Kilowatts: A Review of Small Wind Turbine Applications, Lessons From The US to Brazil», *Sustainability*, vol. 12, n. 7, Art. n. 7, gen. 2020, doi: 10.3390/su12072760.
[4] J.-L. Duchaud, G. Notton, A. Fouilloy, and C. Voyant, «Hybrid renewable power plant sizing – Graphical decision tool, sensitivity analysis and applications in Ajaccio and Tilos», *Appl. Energy*, vol. 254, pag. 113601, nov. 2019, doi: 10.1016/j.apenergy.2019.113601.

[5] Mercer, A S; Bossanyi, E A, «Stall regulation of variable speed HAWTs», [Online]. Disponibile su: https://www.osti.gov/etdeweb/biblio/634821
[6] F. Papi, A. Nocentini, G. Ferrara, and A. Bianchini, «On the Use of Modern Engineering Codes for Designing a Small Wind Turbine: An Annotated Case Study», *Energies*, vol. 14, n. 4, Art. n. 4, gen. 2021, doi: 10.3390/en14041013.
[7] Burton, T., Ed.; J. Wiley, *Wind Energy Handbook*. 2001.
[8] IEC: International Standard, «61400-2 Wind turbines – Part 2: Design requirements for small wind turbines». 2019.
[9] NREL, «OpenFAST code». 2022. Consultato: 28 gennaio 2022. [Online]. Disponibile su: https://www.nrel.gov/wind/nwtc/fast.html
[10] B. Montgomerie, «Methods for Root Effects, Tip Effects and Extending the Angle of Attack Range to +-100 deg, with Application to Aerodynamics for Blades on Wind Turbines and Propellers». FOI Swedish Defense Research Agency, 2004.
[11] C. Bak e P. B. Andersen, «Three-Dimensional Corrections of Airfoil Characteristics Based on Pressure Distributions».
[12] F. Papi, A. Nocentini, P. F. Melani, and A. Bianchini, «Impact Of Post-Stall Extrapolation And Rotational-Augmentation Models On The Performance Of Stall-Controlled Wind Turbines», 2022.
[13] J. Jonkman, S. Butterfield, W. Musial, and G. Scott, «Definition of a 5-MW Reference Wind Turbine for Offshore System Development», NREL/TP-500-38060, 947422, feb. 2009. doi: 10.2172/947422.
[14] E. Gaertner *et al.*, «IEA Wind TCP Task 37: Definition of the IEA 15-Megawatt Offshore Reference Wind Turbine», National Renewable Energy Lab. (NREL), Golden, CO (United States), NREL/TP-5000-75698, mar. 2020. doi: 10.2172/1603478.
[15] MExtremes. Available online: https://www.nrel.gov/wind/nwtc/mextremes.html (accessed on February 2022)
[16] L. Ferrari, G. Soldi, A. Bianchini, E. Dalpane, «Statistical analysis of component failures: A 16 year survey on more than 550 wind turbines» 2018 J. Eng. Gas Turb. Power, 140 (12), 2018, art. no. 121012.